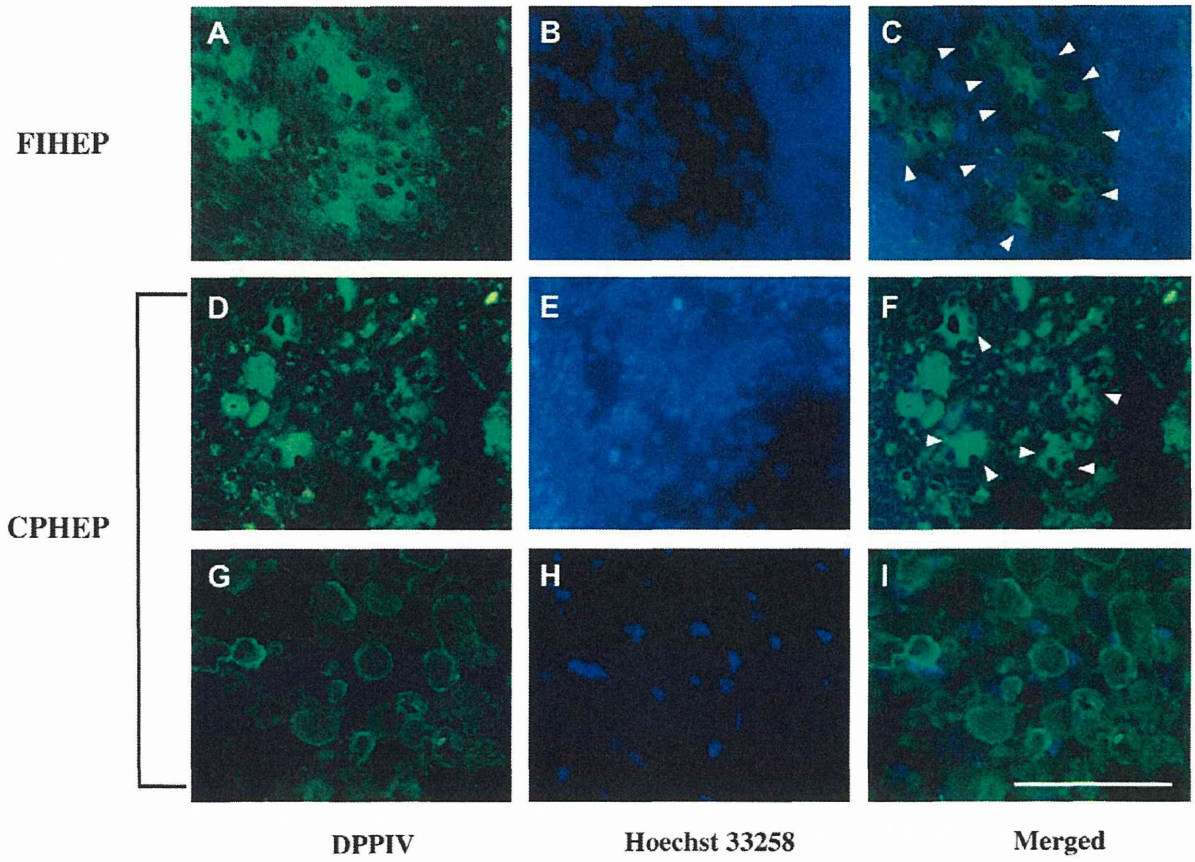

FIG. 3. Engraftment of the transplanted hepatocytes in the spleen of ALF rats. The rats were transplanted with FIHEPs (A)–(C) or CPHEPs (D)–(I) and subjected to ALF as in Figure 2B. Spleens were removed at 24 h after ALF induction and processed to cryosectioning for immunohistochemical analysis to detect DPPIV (green; A, D, G). The sections were counterstained with Hoechst 33258 [blue; (B), (E), (H)]. (A) and (B), (D) and (E), and (G) and (H) were merged into (C), (F), and (I), respectively. The arrowhead indicates $DPPIV^+$/Hoechst 33258^+ viable hepatocytes. Bar, 100 μm.

Blood Chemistry

Hepatocyte transplantation therapy for ALF was evaluated by measuring the blood levels of total bilirubin, GOT, GPT, NH_3, and Glu. The rats in the CM group showed higher levels of total bilirubin, GOT, GPT, and NH_3, and lower levels of Glu, than the hepatocyte-transplanted groups at 24 h post-ALF induction (Fig. 4), indicating that the rats experienced severe liver failure. FIHEP transplantation improved these biochemical data. The CPHEP groups showed improvement to an extent similar to the FIHEP groups. Total bilirubin and NH_3 values improved significantly, which strongly suggests that both engrafted FIHEPs and CPHEPs are functional in cholestasis and NH_3 metabolisms in ALF. However, neither FIHEP nor CPHEP transplantation significantly improved the levels of transaminase, suggesting that the transplanted hepatocytes were not sufficient to prevent ischemic changes induced by ligation of the liver lobes.

Concentrations of inflammatory cytokines in sera were also determined at 24 h post-ALF induction. TGF-β1 measured approximately 7 ng/mL, but IL-1β and IL-6 were not detected in sham-operated rats (Table 1). IL-1β and IL-6 levels in the CM group rose to approximately 300 pg/mL and 4000 pg/mL, respectively. TGF-β1 concentration in the CM group was approximately two times higher than that in sham-operated rats. IL-6 and TGF-β1 concentrations in the FIHEP and CPHEP groups became significantly lower than those in the CM group, although IL-1β concentration did not (Table 1).

Proliferation of the Remnant Liver Hepatocytes Post-ALF Induction

Hepatocyte transplantation increased the host's lifespan, suggesting that the hepatocytes in the remnant liver might be stimulated to proliferate or their cell death rates might decrease despite no gain in liver

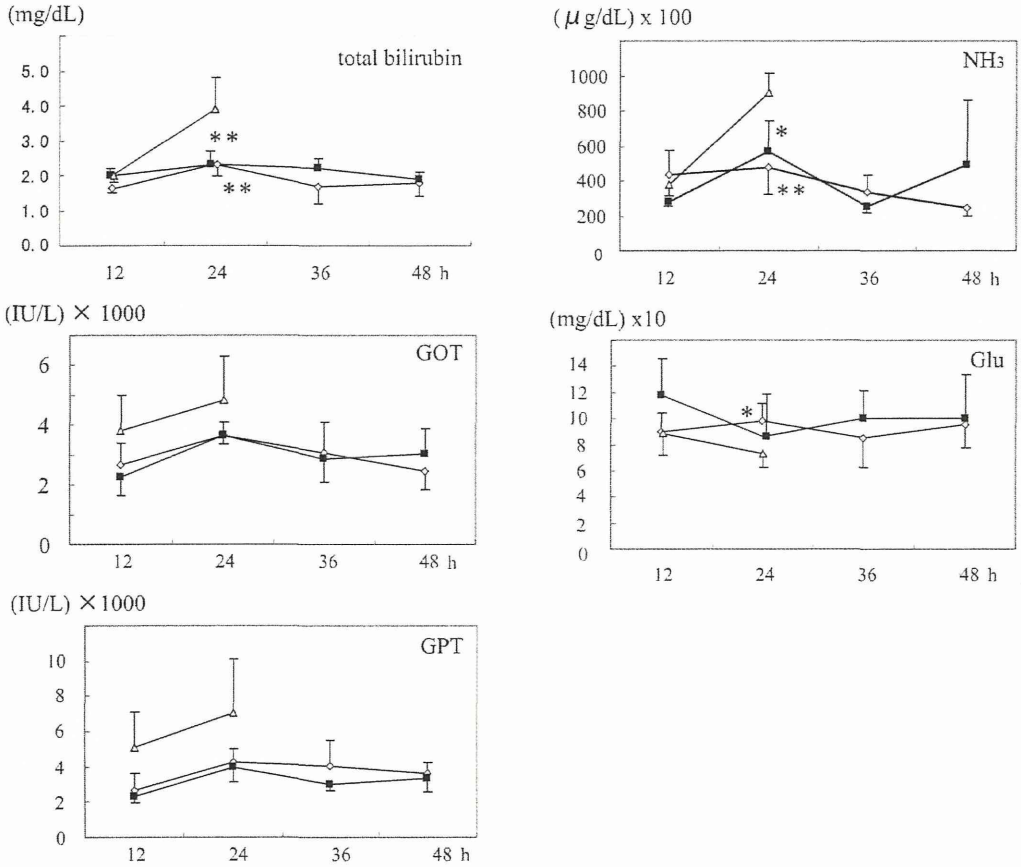

FIG. 4. Biochemical evaluation of hepatocyte transplantation therapy for ALF. The rats were subjected to hepatocyte transplantation and ALF treatment as described in Figure 2. At the indicated time points after ALF treatment, blood was collected for total bilirubin, NH_3, GOT, Glu, and GPT assessment. The mean values of total bilirubin, GOT, GPT, NH_3, and Glu in the normal control rats were 0.3 ± 0.1 (mg/dL), 75 ± 18 (IU/L), 25 ± 6 (IU/L), 151 ± 23 (μg/dL), and 197 ± 26 (mg/dL), respectively. The open diamond, closed rectangle, and open triangle indicate the FIHEP, CPHEP, and CM groups, respectively. *$P < 0.05$ *versus* the CM group. **$P < 0.01$ *versus* the CM group.

weight within the experimental period (up to 5 d). To address this possibility, the BrdU-labeling index and TUNEL activity were determined as a measure of cell proliferation activity and cell death, respectively. BrdU-labeling indexes at 24 h post-ALF in the CM, FIHEP, and CPHEP groups are shown in Figure 5A-1, A-2, and A-3, respectively. $BrdU^+$ nuclei were present in the FIHEP and CPHEP groups but were scarce in the CM group. These $BrdU^+$ hepatocytes were host hepatocytes because they were $DPPIV^-$. The BrdU-labeling indexes are shown in Figure 5A-4. The indexes at 12 h were low (<2%) and not significantly different among the three groups of rats. The indexes of the FIHEP and CPHEP groups at 24 h significantly increased, compared with those of the CM group. At 48 h post-ALF, there was a similarly large increase in the labeling indexes (>10%) in both the FIHEP and CPHEP rat livers, indicating that CPHEP transplantation stimulated the proliferation of the remnant hepatocytes as effectively as FIHEP transplantation. In a parallel experiment, some sections at 24 h post-ALF were stained for TUNEL activity. $TUNEL^+$ hepatocytes were frequently observed in the CM rats (Fig. 5B-1) but decreased substantially in the FIHEP (Fig. 5B-2) and CPHEP (Fig. 5B-3) rats. The ratios of the $TUNEL^+$ hepatocytes to the total hepatocytes are shown in Figure 5B-4 as apoptotic indexes. The apoptotic index

TABLE 1

Comparison of Inflammatory Cytokines 24 h Post-ALF Induction

Exp. group	IL-1β (pg/mL)	IL-6 (pg/mL)	TGF-β1 (ng/mL)
SO	ND	ND	7.27 ± 3.16
FIHEP	382.1 ±107.3	499.8 ± 485.6	10.56 ± 4.21*
CPHEP	418.1 ± 73.8	337.4 ± 150.7*	10.79 ± 1.94*
CM	329.1 ± 32.8	4375.5 ± 5568.9	15.27 ± 2.74

ALF = acute liver failure; SO = sham operation; ND = not detected. FIHEP = freshly isolated hepatocyte; CPHEP = culture-propagated hepatocyte; CM = culture medium

Sham operation indicates laparotomy alone.

*$P < 0.05$ *versus* the CM group.

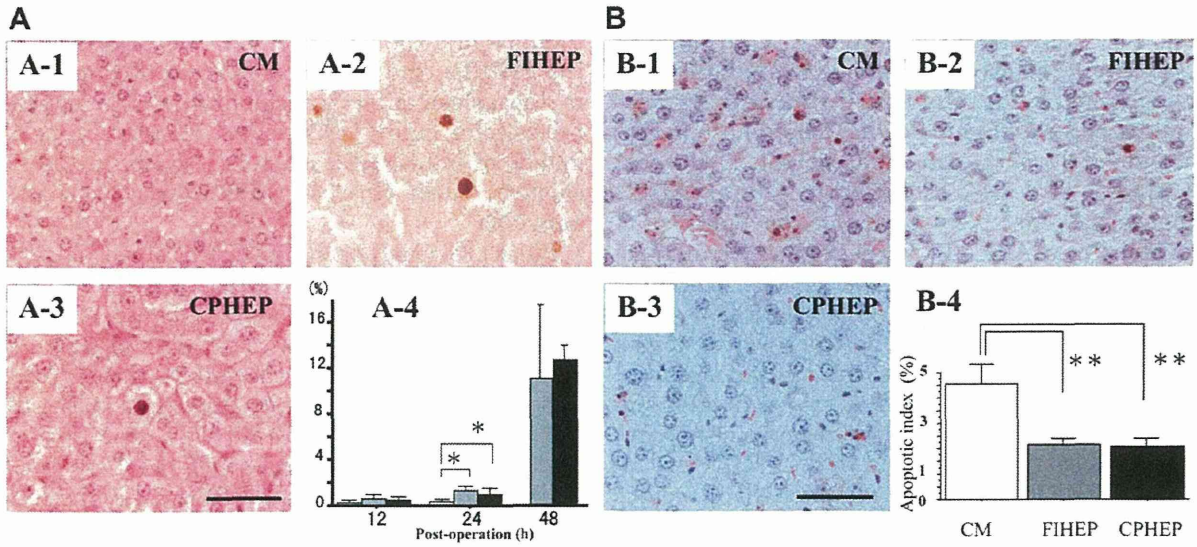

FIG. 5. (A) BrdU-labeling index of hepatocytes in the remnant liver of the hepatocyte- transplanted rat. The rats were injected with CM, transplanted with FIHEPs or CPHEPs, and subjected to ALF as in Fig. 2. The remnant livers (omental lobe) were removed at 12, 24, and 48 h post-induction of ALF and processed to obtain paraffin sections for BrdU staining. (A-1), (A-2), and (A-3) are representative of photos from rats with CM, FIHEPs, and CPHEPs, respectively, taken at 24 h post-ALF. $BrdU^-$ nuclei are brown in color. In (A-4), $BrdU^+$ cells were counted from five microscopic fields of each section from 4 rats in each group at the time points indicated, and the BrdU-labeling index was calculated as the ratio of $BrdU^+$ cells to the total cells in a counted field. The open bar, gray bar, and black bar indicate the CM, FIHEP, and CPHEP groups, respectively. $*P < 0.05$ *versus* the CM group. Bar, 50 μm. (B) Suppression of remnant hepatocyte apoptosis by hepatocyte transplantation. The rats were transplanted with hepatocytes and subjected to ALF as described in Fig. 2. Paraffin sections were prepared from the remnant livers (omental lobes) isolated from the CM (B-1), FIHEP (B-2), and CPHEP groups (B-3) at 24 h post-ALF and were stained for TUNEL activity. $TUNEL^+$ pycnotic nuclei (brown) were frequently observed in the CM group, but less often in the FIHEP and CPHEP groups. Apoptotic cells were counted from five microscopic fields of liver tissue sections from four rats in each group. The ratio of apoptotic cells to total cells in the counted field was expressed as the apoptotic index (B-4). The open bar, gray bar, and black bar indicate the CM, FIHEP, and CPHEP groups, respectively. $**P < 0.01$ *versus* the CM group. Bar, 50 μm.

of the remnant liver in the FIHEP and CPHEP groups decreased to approximately 50% of that in the CM group. These $TUNEL^+$ hepatocytes were host hepatocytes because they were $DPPIV^-$. Thus, CPHEP transplantation suppressed the apoptotic changes in the host hepatocytes as effectively as FIHEP transplantation.

DISCUSSION

Although several studies have supported the effectiveness of hepatocyte transplantation in treating patients with ALF, there is a severe problem in using hepatocyte transplantation therapy as a general clinical treatment for patients with liver failure: owing to the lack of donor organs available for clinical use, hospitals cannot supply sufficient quantities of normal human hepatocytes to such patients. One way to overcome this limitation might be to devise a method of abundantly propagating hepatocytes in culture, starting with a small amount of hepatocytes isolated from small pieces of available liver tissues. However, it does not seem to be a practical solution, because it is well documented that normal hepatocytes show poor multiplication ability *in vitro* despite their remarkable growth potential *in vivo* [19].

We have been engaged in developing a technology to abundantly propagate hepatocytes in culture [8, 9] and previously reported that rat hepatocytes were capable of repeatedly multiplying *in vitro* when cocultured with Swiss 3T3 cells in a medium that we devised [10]. We have now shown that such CPHEPs can be used as a source of hepatocyte transplantation for preventing hepatectomy-induced ALF. Resection of hepatic tumors is currently the gold standard treatment for patients with either primary or secondary liver malignancies. An extended hepatectomy is often necessary to achieve curative resection; however, ALF after massive hepatectomy remains a challenging problem (i.e., the risk of insufficiency of remnant liver volume, leading to unresectability). If we devise a countermeasure to prevent ALF beforehand, aggressive hepatic resection could be safely performed. Seeking to answer this clinical question, we evaluated the prevention efficacy of CPHEP transplantation in a surgical model of hepatectomy-induced ALF.

To estimate the efficacy of transplanting either FIHEPs or CPHEPs in ALF, we employed an experimental ALF model induced by subjecting rats to two-thirds-hepatectomy and ligation of the right-lobe pedicle. This method induces more severe liver failure than

a model induced by 90% hepatectomy and is considered to mimic the clinical status of human ALF fairly faithfully [14]. The rats lacked a functional liver and showed ischemic changes in the right lobe, resulting in regeneration failure of the remnant omental lobe, whose weight occupied about 8% of the total liver weight. This model has previously been used to demonstrate that FIHEP transplantation effectively prolongs the survival of rats suffering from ALF [15]. We reproduced similar results in the present study. Notably, CPHEPs, which had been prepared by multiplying FIHEPs 3 times, were as effective as FIHEPs in prolonging the survival of rats suffering from ALF. CPHEP transplantation improved all the liver functions tested in this study. In addition, the BrdU-labeling index of the hepatocytes in the remnant liver was comparable to that in the FIHEP group. Rats with CPHEPs gradually regained liver weight after ALF induction, as did those with FIHEPs. These results together indicate that both CPHEP and FIHEP could be a source for hepatocyte transplantation to promote regeneration of the remnant liver after ALF induction.

There have been two explanations for lethal hepatic failure after excessive hepatectomy: hepatectomy causes microcirculer disturbances [20] or induces cytotoxic factors such as TNF-α, TGF-β1, and oxidative stress-related factors [21, 22]. In the present study, we did not find any evidence of microvascular disturbances on hematoxylin and eosin (H&E)-stained sections of the remnant lobe in the ALF-induced rats, but we did observe hypercytokinemia of cytokines such as IL-6 and TGF-β1. Apoptotic hepatocytes were frequently seen by TUNEL assay in the remnant liver lobe of the ALF-induced rats. CPHEP and FIHEP transplantation decreased the concentrations of IL-6 and TGF-β1 in sera, as well as the frequency of apoptotic hepatocytes. Therefore, it appears that both CPHEPs and FIHEPs prolonged the survival of ALF-induced rats by suppressing the hepatocytic apoptosis in the remnant liver.

In the present study, we demonstrated the presence of DPPIV$^+$ hepatocytes in the spleen at 24 h after ALF induction, which clearly indicated the engraftment of both transplanted CPHEPs and FIHEPs in the graft site. There were no significant differences in the frequency of DPPIV$^+$ hepatocytes between the FIHEP and CPHEP groups. However, the expression level of hepatocyte-specific mRNAs such as Alb, CYP2C7, and GS in the spleen of the CPHEP rats was considerably lower than that in the FIHEP rats. This might be explained by the fact that CPHEPs showed lower expression levels of these marker genes than FIHEPs at the time of transplantation; this was due to the fact that the CPHEP cells had been cultured for 11 d before transplantation, during which time the expression levels had decreased (Fig. 1B). Another explanation could be that the CPHEPs were more vulnerable than the FIHEPs, and that most of them became nonviable in the spleen after transplantation. We noticed the presence of many DPPIV$^+$ but Hoechst$^-$ cells in the middle of the CPHEP clusters, but not in the FIHEP clusters. These Hoechst$^-$ cells were considered to be nonviable.

It has previously been shown that homogenized hepatocytes were even effective as a treatment for liver failure [23], suggesting the effectiveness of nonviable hepatocytes. In the present study, we also showed that the survival rate of the rats in the DHEP group was better, to some extent, than that in the control CM group, although the rate was much lower than that of the CPHEP group. In light of these results, it is likely that transplanted CPHEPs contribute to the improvement of liver failure by substituting the function of the host liver. They may also provide some growth factors or enzymes to support the regeneration of the remnant liver. It remained to be elucidated whether the cryopreserved CPHEPs also display such beneficial effects. Hepatocytes are known to be very sensitive to freezing damage. Three distinct modes of cryopreservation-induced hepatocyte death have been identified, namely, physical cell rupture, necrosis, and apoptosis [24]. The susceptibility of hepatocytes to such freeze-thaw injury is attributed to the damage to mitochondria, including loss of mitochondrial membrane integrity, increase in membrane permeability, etc. The inhibition of mitochondria damage, for instance, by broad-spectrum caspase-inhibitor, would prevent cryopreservation-induced damage of propagated hepatocytes.

In conclusion, the transplantation of homologous CPHEPs has a remarkable therapeutic potential for ALF in rats. Since we have recently established a culture method that enables us to multiply human hepatocytes 50 to 100 times during 50 d of culture [25], CPHEPs might be a useful source of hepatocytes for transplantation to treat human patients with ALF.

REFERENCES

1. Lee WM. Acute liver failure. N Engl J Med 1993;329:1862.
2. Bismuth H, Samuel D, Casting D, et al. Orthotopic liver transplantation in fulminant and subfulminant hepatitis. Ann Surg 1995;222:109.
3. Moreno GE, Garcia GI, Loinaz SC, et al. Liver transplantation in patients with fulminant hepatic failure. Br J Surg 1995;82:118.
4. Gewartowska M, Olszewski WL. Hepatocyte transplantation-biology and application. Ann Transplant 2007;12:27.
5. Habibullah MC, Syde HI, Qamar A, et al. Human fetal hepatocyte transplantation in patients with fulminant hepatic failure. Transplantation 1994;58:951.
6. Strom SC, Fisher RA, Thompson MT, et al. Hepatocyte transplantation as a bridge to orthotopic liver transplantation in terminal liver failure. Transplantation 1997;63:559.

7. Fisher RA, Bu D, Thompson M, et al. Defining hepatocellular chimerism in liver failure patient bridge with hepatocyte infusion. Transplantation 2000;69:303.
8. Tateno C, Yoshizato K. Long-term cultivation of adult rat hepatocytes that undergo multiple cell divisions and express normal parenchymal phenotypes. Am J Pathol 1996;148:383.
9. Tateno C, Takai-Kajihara K, Yamasaki C, et al. Heterogeneity of growth potential of adult rat hepatocytes *in vitro*. Hepatology 2000;31:65.
10. Sato H, Funahashi M, Kristensen DB, et al. Pleiotrophin as a Swiss 3T3 cell-derived potent mitogen for adult rat hepatocytes. Exp Cell Res 1999;246:152.
11. Hino H, Tateno C, Sato H, et al. A long-term culture of human hepatocytes which show a high growth potential and express their differentiated phenotypes. Biochem Biophys Res Commun 1999;256:184.
12. Seglen PO. Preparation of isolated rat liver cells. Methods Cell Biol 1976;13:29.
13. Katayama S, Tateno C, Asahara T, et al. Size-dependent *in vivo* growth potential of adult rat hepatocytes. Am J Pathol 2001; 158:97.
14. Eguchi S, Lilja H, Hewitt W, et al. Loss and recovery of liver regeneration in rats with fulminant hepatic failure. J Surg Res 1997;72:112.
15. Eguchi S, Kamolt A, Ljubiova J, et al. Fulminant hepatic failure in rats: Survival and effects on blood chemistry and liver regeneration. Hepatology 1996;24:1452.
16. Higgins GM, Anderson RM. Experimental pathology of the liver. 1. Restoration of the liver of the white rat following partial surgical removal. Arch Pathol 1931;12:186.
17. Gordon GJ, Coleman WB, Hixon DC, et al. Liver regeneration in rats with retrosine-induced hepatocellular injury proceeds through a novel cellular response. Am J Pathol 2000; 156:607.
18. Asahina K, Sato H, Yamasaki C, et al. Pleiotrophin/heparin-binding growth-associated molecule as a mitogen of rat hepatocytes and its role in regeneration and development of liver. Am J Pathol 2002;160:2191.
19. Fausto N, Campbell JS, Riehle KJ. Liver regeneration. Hepatology 2006;43(2 Suppl. 1):45.
20. Kamimukai N, Togo S, Hasegawa S, et al. Expression of Bcl-2 family reduces apoptotic hepatocytes after excessive hepatectomy. Eur Surg Res 2001;33:8.
21. Leist M, Gantner F, Bohlinger I, et al. Tumor necrosis factor-induced hepatocyte apoptosis precedes liver failure in experimental murine shock models. Am J Pathol 1995;146:1220.
22. Oberhammer FA, Pavelka M, Sharma S, et al. Induction of apoptosis in culture hepatocytes and in regressing liver by transforming growth factor β1. Proc Natl Acad Sci U S A 1992; 89:5408.
23. Grundmann R, Koebe HG, Waters W. Transplantation of cryopreserved hepatocytes or liver cytosol injection in the treatment of acute liver failure in rats. Res Exp Med 1986; 186:141.
24. Terry C, Dhawan A, Mitry RR, Hughes RD. Cryopreservation of isolated human hepatocytes for transplantation: State of the art. Cryobiology 2006;53:149.
25. Yamasaki C, Tateno C, Aratani A, et al. Growth and differentiation of colony-forming human hepatocytes in vitro. J Hepatol 2006;44:749.

Biochemical and Biophysical Research Communications 440 (2013) 515–520

Contents lists available at ScienceDirect

Biochemical and Biophysical Research Communications

journal homepage: www.elsevier.com/locate/ybbrc

Specific inhibition of hepatitis C virus entry into host hepatocytes by fungi-derived sulochrin and its derivatives

Syo Nakajima [a,b], Koichi Watashi [a,b,*], Shinji Kamisuki [b], Senko Tsukuda [a,c], Kenji Takemoto [b], Mami Matsuda [a], Ryosuke Suzuki [a], Hideki Aizaki [a], Fumio Sugawara [b], Takaji Wakita [a]

[a] Department of Virology II, National Institute of Infectious Diseases, Tokyo 162-8640, Japan
[b] Tokyo University of Science Graduate School of Science and Technology, Noda 278-8510, Japan
[c] Micro-Signaling Regulation Technology Unit, RIKEN Center for Life Science Technologies, Wako 351-0198, Japan

ARTICLE INFO

Article history:
Received 5 September 2013
Available online 5 October 2013

Keywords:
HCV
Entry
Sulochrin
Natural product
Screening
Compound

ABSTRACT

Hepatitis C virus (HCV) is a major causative agent of hepatocellular carcinoma. Although various classes of anti-HCV agents have been under clinical development, most of these agents target RNA replication in the HCV life cycle. To achieve a more effective multidrug treatment, the development of new, less expensive anti-HCV agents that target a different step in the HCV life cycle is needed. We prepared an in-house natural product library consisting of compounds derived from fungal strains isolated from seaweeds, mosses, and other plants. A cell-based functional screening of the library identified sulochrin as a compound that decreased HCV infectivity in a multi-round HCV infection assay. Sulochrin inhibited HCV infection in a dose-dependent manner without any apparent cytotoxicity up to 50 μM. HCV pseudoparticle and trans-complemented particle assays suggested that this compound inhibited the entry step in the HCV life cycle. Sulochrin showed anti-HCV activities to multiple HCV genotypes 1a, 1b, and 2a. Co-treatment of sulochrin with interferon or a protease inhibitor telaprevir synergistically augmented their anti-HCV effects. Derivative analysis revealed anti-HCV compounds with higher potencies ($IC_{50} < 5$ μM). This is the first report showing an antiviral activity of methoxybenzoate derivatives. Thus, sulochrin derivatives are anti-HCV lead compounds with a new mode of action.

1. Introduction

Hepatitis C virus (HCV) infection is a major causative agent of chronic liver diseases such as liver cirrhosis and hepatocellular carcinoma [1]. The standard anti-HCV therapy has been a co-treatment with pegylated-interferon (IFN)α and ribavirin, but this therapy is limited by less efficacy to certain HCV genotypes, poor tolerability, serious side effects, and high cost [2,3]. In addition to the newly approved protease inhibitors, telaprevir and boceprevir, a variety of anti-HCV candidates are under clinical development. Although these drugs improve the virological response rate, the emergence of drug-resistant virus is expected to be a significant problem. Moreover, these compounds are expensive due to their complex structure and the many steps required for their total synthesis. To overcome the drug-resistant virus and achieve a long-term antiviral effect, multidrug treatment is essential. Thus, the development of drugs targeting a different step in the HCV life cycle and presumably requiring low cost is urgently needed.

HCV propagates in hepatocytes through its viral life cycle including: attachment and entry (defined as the early step in this study); translation, polyprotein processing, and RNA replication (the middle step); and assembly, trafficking, budding, and release (the late step) (Supplementary Fig. S1). The middle step has been extensively analysed, especially after the establishment of the HCV replicon system [4]. The early step can be analysed with HCV pseudoparticle (HCVpp) [5,6], which is a murine leukemia virus- or human immunodeficiency virus-based pseudovirus carrying HCV E1 and E2 as envelope proteins. The HCV-producing cell culture system (HCVcc) is used for analyzing the whole life cycle [7–9]. In addition, the HCV trans-complemented particle (HCVtcp) system carrying an HCV subgenomic replicon RNA packaged in HCV E1 and E2-containing particles can evaluate the life cycle from the early to the middle step [10]. The majority of anti-HCV agents currently under clinical development, such as inhibitors of protease, polymerase, NS5A, and cellular cyclophilin, inhibit polyprotein processing and/or RNA replication. A desirable approach

Abbreviations: HCV, hepatitis C virus; IFN, interferon; HCVpp, HCV pseudoparticle; HCVcc, HCV derived from cell culture; HCVtcp, HCV trans-complemented particle; MOI, multiplicity of infection; HBs, HBV envelope protein; CsA, cyclosporin A; VSV, vesicular stomatitis virus.

* Corresponding author. Adress: Department of Virology II, National Institute of Infectious Diseases, 1-23-1 Toyama, Shinjuku-ku, Tokyo 162-8640, Japan. Fax: +81 3 5285 1161.
E-mail address: kwatashi@nih.go.jp (K. Watashi).

0006-291X/$ - see front matter © 2013 Elsevier Inc. All rights reserved.
http://dx.doi.org/10.1016/j.bbrc.2013.09.100

to achieving efficient multidrug therapy is to identify new antiviral drugs targeting different steps in the viral life cycle. A combination of drugs with different targets can greatly decrease the emergence of drug-resistant virus.

Natural products generally contain more characteristics of high chemical diversity than combinatorial chemical collections, and therefore have a wider range of physiological activities [11,12]. They offer major opportunities for finding novel lead structures that are active in a biological assay. Moreover, biologically active natural products are generally small molecules with drug-like properties, and thus development costs of producing orally active agents tend to be lower than that derived from combinatorial chemistry [13]. In addition, there is a wide variety of natural compounds reported to possess antiviral activity [14,15]. In the present study, we have taken advantage of the potential of natural products by screening a natural product library derived from fungal extracts with a cell-based assay that supports the whole life cycle of HCV.

2. Materials and methods

2.1. Cell culture

Huh-7.5.1 [8] and HepaRG cells [16] were cultured as described previously.

2.2. Natural product library and reagents

Natural products were extracted essentially as previously described [17]. Culture broths of fungal strains isolated from seaweeds, mosses, and other plants were extracted with CH_2Cl_2. The crude extracts were separated by silica gel column chromatography to purify compounds. The chemical structure of each compound was determined by NMR and mass spectrometry analyses. Thus, we prepared an in-house natural product library consisting of approximately 300 isolated compounds.

Cyclosporin A was purchased from Sigma. Bafilomycin A1 and chlorpromazine were purchased from Wako. Heparin was obtained from Mochida Pharmaceutical. IFNα was purchased from Schering-Plough.

2.3. Compound screening

Huh-7.5.1 cells were treated with HCV J6/JFH1 at a multiplicity of infection (MOI) of 0.15 for 4 h. The cells were washed and then cultured with growth medium treated with 10 μM of each compound for 72 h. The infectivity of HCV in the medium was quantified. Cell viability at 72 h post-treatment was simultaneously measured. Compounds that decreased the cell viability to less than 50% of that without treatment were eliminated for further evaluations. Normalised infectivity was calculated as HCV infectivity divided by cell viability. Compounds reducing the normalised infectivity to less than 40% were selected as initial hits. The initial hits were further evaluated for data reproduction and dose-dependency.

2.4. HCVcc assay

HCVcc was recovered from the medium of Huh-7.5.1 cells transfected with HCV J6/JFH-1 RNA as described [7]. HCVcc was infected into Huh-7.5.1 cells at 0.15 MOI for 4 h. After washing out the inoculated virus, the cells were cultured with normal growth medium in the presence or absence of compounds for 72 h. The infectivity of HCV and the amount of HCV core protein in the medium were quantified by infectious focus formation assay and chemiluminescent enzyme immunoassay (Lumipulse II HCV core assay, ortho clinical diagnostics), respectively [7,18].

2.5. Immunoblot analysis

Immunoblot analysis was performed as described previously [19]. The anti-HCV core antibody (2H9) was used as a primary antibody with 1:1000 dilution [7].

2.6. MTT assay

The viability of cells was quantified by using a Cell Proliferation Kit II XTT (Roche Diagnostics) as described previously [20].

2.7. HCV replicon assay

Huh-7.5.1 cells were transfected with an HCV subgenome replicon RNA (SGR–JFH1/Luc) for 4 h and then incubated with or without compounds for 48 h [21]. The cells were lysed with 1xPLB (Promega), and the luciferase activity was determined with a luciferase assay system (Promega) according to the manufacturer's protocol [22].

2.8. HCVpp assay

HCVpp was recovered from the medium of 293T cells transfected with expression plasmids for HCV JFH-1 E1E2, MLV Gag-Pol, and luciferase, which were kindly provided from Dr. Francois-Loic Cosset at Universite de Lyon [5]. Vesicular stomatitis virus pseudoparticles (VSVpp) was similarly recovered with transfection by replacing HCV E1E2 with VSV G.

Huh-7.5.1 cells were preincubated with compounds for 3 h and were then infected with HCVpp in the presence of compounds for 4 h. After washing out virus and compounds, cells were incubated for an additional 72 h before recovering the cell lysates and quantifying the luciferase activity.

2.9. HCVtcp assay

The HCVtcp assay was essentially performed as described [10]. Briefly, Huh-7 cells were transfected with expression plasmids for the HCV subgenomic replicon carrying the luciferase gene and for HCV core-NS2 based on genotype 1a (RMT) (kindly provided by Dr. Michinori Kohara at Tokyo Metropolitan Institute of Medical Science), 1b (Con1), and 2a (JFH-1) [4,10,23] to recover HCVtcp. HCVtcp can reproduce RNA replication as well as HCV-mediated entry into the cells [10].

2.10. Synergy analysis

To determine whether the effect of the drug combination was synergistic, additive, or antagonistic, MacSynergy (kindly provided by Mark Prichard), a mathematical model based on the Bliss independence theory, was used to analyse the experimental data shown in Fig. 3A. In this model, a theoretical additive effect with any given concentrations can be calculated by $Z = X + Y(1-X)$, where X and Y represent the inhibition produced by each drug alone, and Z represents the effect produced by the combination of two compounds if they were additive. The theoretical additive effects were compared to the actual experimental effects at various concentrations of the two compounds and were plotted as a three-dimensional differential surface that would appear as a horizontal plane at 0 if the combination were additive. Any peak above this plane (positive values) indicates synergy, whereas any depression below the plane (negative values) indicates antagonism. The 95% confidence interval of the experimental dose–response was considered to reveal only effects that were statistically significant.

3. Results

3.1. Screening of natural products possessing anti-HCV activity

We extracted culture broths of fungal strains isolated from seaweeds, mosses, and other plants and purified compounds as described in the Section 2 [17]. The chemical structure of each compound was determined by NMR and mass spectrometry analyses. Thus, we prepared an in-house natural product library consisting of approximately 300 isolated compounds. As shown in the Section 2, compounds reducing the normalised HCV infectivity to less than 40% as compared with DMSO were selected as primary hits. The primary hits were then validated by examining the reproducibility, dose-dependency, and cell viability in the HCVcc system. Sulochrin [methyl 2-(2,6-dihydroxy-4-methylbenzoyl)-5-hydroxy-3-methoxybenzoate] (Fig. 1A) was one of the compounds showing the highest anti-HCV activity, and the following analyses focus mainly on this compound.

3.2. Sulochrin decreased HCV infectivity in HCV cell culture assay

To characterise the anti-HCV activity of the compounds, Huh-7.5.1 cells were infected with HCV J6/JFH1 at an MOI of 0.15 and then cultured for 72 h in the presence or absence of compounds.

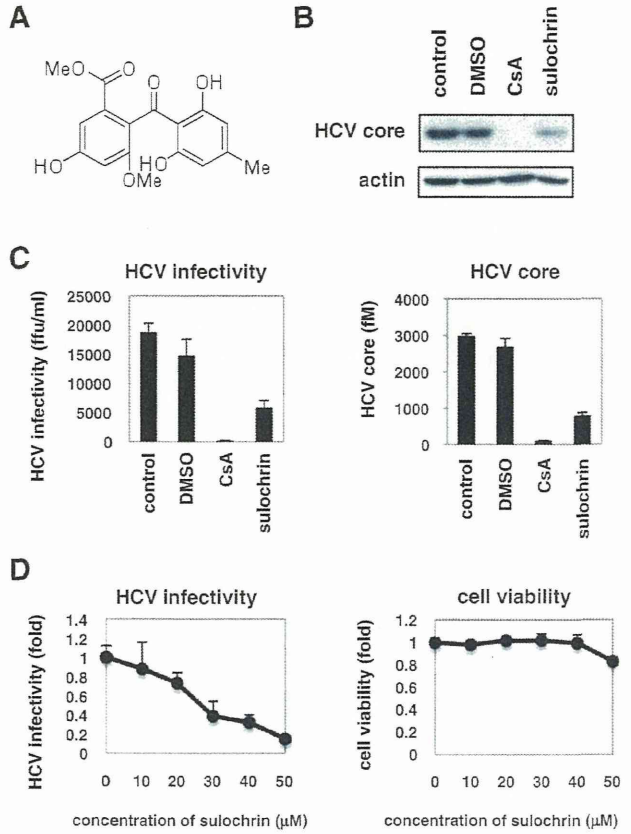

Fig. 1. Sulochrin decreased HCV production in a multi-round HCV infection assay. (A) Chemical structure of sulochrin. (B) Huh-7.5.1 cells were infected with HCV J6/JFH-1 at an MOI of 0.15 for 4 h and then incubated with or without 0.3% DMSO, 2 μM cyclosporin A (CsA), or 30 μM sulochrin for 72 h. The resultant medium was inoculated into naïve Huh-7.5.1 cells to detect intracellular HCV core and actin protein at 48 h postinoculation by immunoblot. (C) HCV infectivity (left) and HCV core protein (right) in the medium as prepared in (B) were quantified as shown in the Section 2. (D) HCV infectivity (left) determined as shown in (C) with varying concentrations (0–50 μM) of sulochrin. Cell viability was examined by MTT assay (right).

In this system, infectious HCV is secreted into the medium and then re-infects into uninfected cells to support the spread of HCV during a 72 h period (Section 2). Cell cultures were treated with sulochrin or cyclosporin A (CsA) as a positive control in this mul-

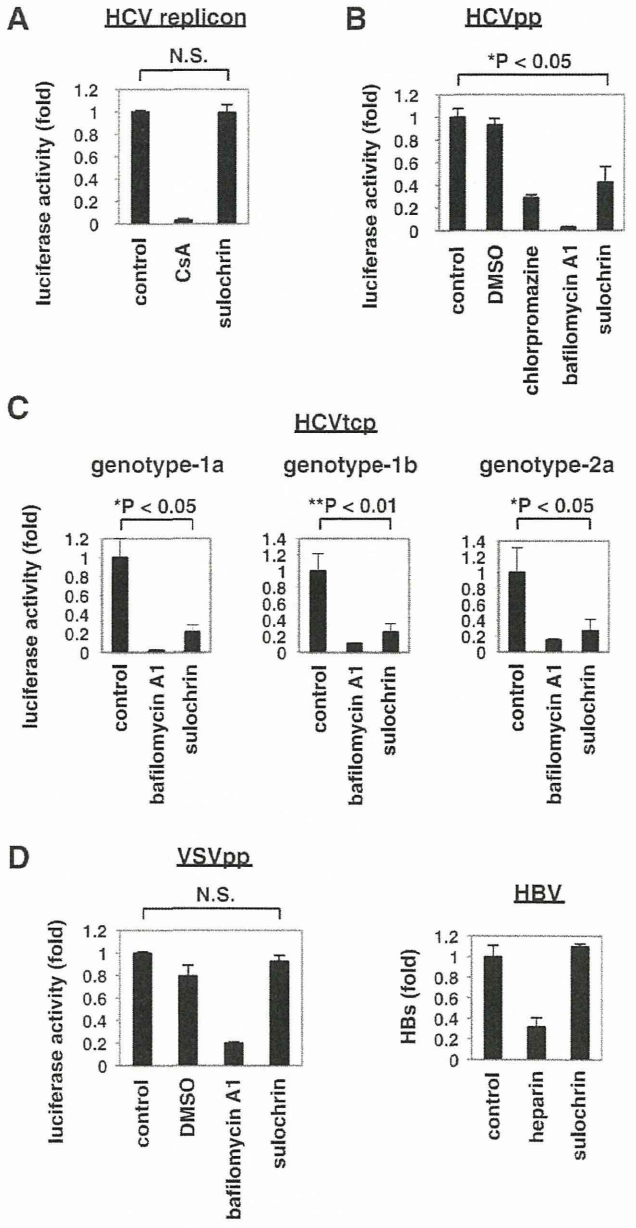

Fig. 2. Sulochrin blocked HCV entry. (A) Replicon assay. Huh-7.5.1 cells were transfected with an HCV subgenomic replicon RNA for 4 h followed by treatment with or without the indicated compounds for 48 h. Luciferase activity driven by the replication of the subgenomic replicon was quantified. (B and C) HCV pseudoparticle (HCVpp) and trans-complemented particle (HCVtcp) assay. Huh-7.5.1 cells were pretreated with the indicated compounds for 3 h and then infected with HCVpp (B) or HCVtcp (C) for 4 h. After washing out virus and compounds, cells were further incubated for 72 h and harvested for measuring luciferase activity driven by the infection of HCVpp or HCVtcp. HCVtcp assay was performed with HCV E1 and E2 derived from genotypes 1a (RMT), 1b (Con1), and 2a (JFH1). (D) Left, the pseudoparticle assay was performed as shown in (B) with VSV G instead of HCV E1 and E2. Right, HBV infection assay. HepaRG cells were pretreated with the indicated compounds for 3 h and then infected with HBV for 16 h. After washing out virus and compounds, cells were incubated for an additional 12 days. HBV infection was evaluated by measuring HBs secretion from the infected cells. Heparin was used as a positive control that inhibits HBV entry.

ti-round infection system. To examine the level of infectious HCV particles produced from the cells, the resultant medium was inoculated into naive Huh-7.5.1 cells to detect HCV core protein in the cells. As shown in Fig. 1B, intracellular production of HCV core but not that of actin was reduced in the cells inoculated with sulochrin- and CsA-treated medium (Fig. 1B). Quantitative analysis showed that sulochrin decreased HCV infectivity and HCV core protein in the medium to 1/3–1/4 of the untreated levels (Fig. 1C). Reduction of HCV infectivity by sulochrin was dose-dependent without serious cytotoxicity up to 50 μM (Fig. 1D).

3.3. Sulochrin blocked HCV entry

We investigated the step in the HCV life cycle that was inhibited by sulochrin. The middle step of the life cycle including translation and RNA replication was evaluated with the transient replication assay by using the HCV subgenomic replicon. Sulochrin had little effect on the replicon activity at doses up to 50 μM (Fig. 2A). In the HCVpp system, which reproduced the early step of HCV infection including entry, sulochrin significantly inhibited HCVpp infection (Fig. 2B). Sulochrin also inhibited the infection of HCVtcp, which reproduced both the viral entry and RNA replication, further supporting that this compound targeted the entry step (Fig. 2C). In contrast, VSV G-mediated viral entry efficiency was not altered by sulochrin treatment (Fig. 2D). Additionally, HBV entry was not inhibited by the presence of sulochrin (Fig. 2D). These data suggest that the inhibitory activity of sulochrin on viral entry is specific to HCV. The anti-HCV entry activity of sulochrin was conserved among different HCV genotypes, 1a (RMT), 1b (Con1), and 2a (JFH-1) [4,10,23] (Fig. 2C).

3.4. Synergistic effect of cotreatment of sulochrin with IFNα or telaprevir

We examined the anti-HCV activity of sulochrin co-administered with clinically available anti-HCV agents, IFNα and a prote-

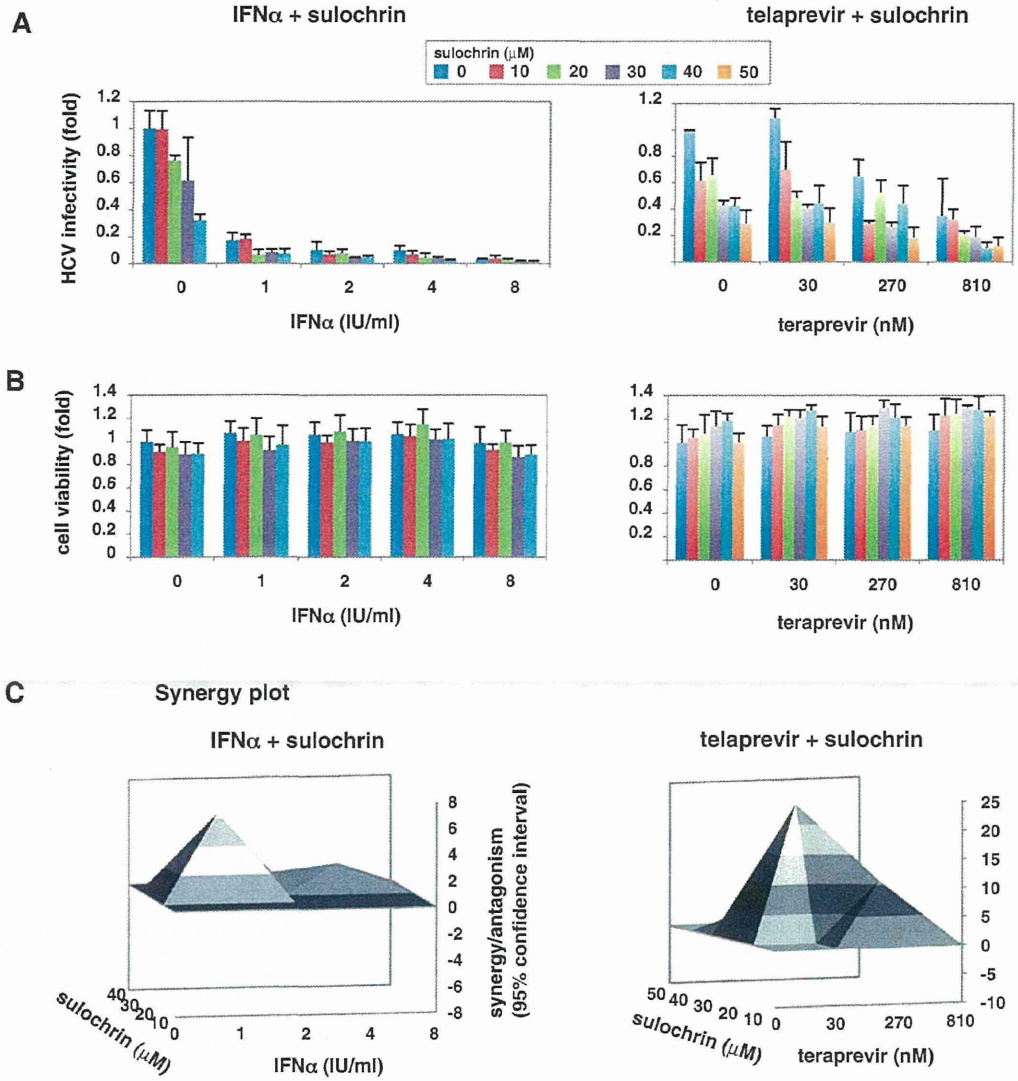

Fig. 3. Cotreatment of sulochrin with IFNα or telaprevir. (A, B) Huh-7.5.1 cells infected with HCV were treated with the indicated concentrations of sulochrin with IFNα (left) or telaprevir (right) to determine HCV infectivity in the medium (A) as shown in Fig. 1C. Cell viability was also quantified (B). (C) Synergy analysis. The results of the combinations shown in (A) were analysed with a mathematical model, MacSynergy, as described in the Section 2. The three-dimensional surface plot represents the difference between actual experimental effects and theoretical additive effects of the combination treatment (95% confidence interval). The theoretical additive effects are shown as the zero plane (dark gray) across the *z*-axis. A positive value in the *z*-axis as a peak above the plane indicates synergy, and a negative value with a valley below the plane indicates antagonism. Sulochrin in combination with IFNα (left) or telaprevir (right) produced synergistic antiviral effects that were greater than the theoretical additive effects.

ase inhibitor telaprevir. As shown in Fig. 3, addition of sulochrin with IFNα or telaprevir led to a further decrease in HCV infectivity (Fig. 3A) without significantly enhancing cytotoxicity (Fig. 3B) at any given concentrations. Thus, the combination of sulochrin and IFNα or telaprevir always resulted in a greater reduction in HCV infectivity as compared with that achieved by either agent alone. Synergy/antagonism analysis with the Bliss independence model showed that the experimental anti-HCV activity in combination with sulochrin and IFNα or telaprevir showed a peak above the zero plane in the *z*-axis, which shows the calculated theoretical additive effect (Fig. 3C). Any peak above the zero plane indicates more than an additive effect, namely, synergy (Section 2). The data clearly indicate that sulochrin had a synergistic anti-HCV effect with both IFNα and telaprevir.

3.5. Derivative analysis of sulochrin

We examined the anti-HCV activity of a series of sulochrin derivatives (Fig. 4A) in the HCVcc system. Monochlorosulochrin and dihydrogeodin, mono- or dichloro-substituted derivatives of sulochrin, possessed even higher anti-HCV activity than sulochrin (Fig. 4B and C). Deoxyfunicone, of which one aromatic ring was replaced by a 4-pyrone ring, had approximately 5-fold greater HCV inhibitory activity as compared with sulochrin (Fig. 4B and C). An additional compound, 3-*O*-methylfunicone, also possessed anti-HCV activity (Fig. 4B and C). These data suggest that the 1,3-dihydroxy-5-methylbenzene moiety of sulochrin is important for anti-HCV activity. Furthermore, funicone derivatives as well as sulochrin derivatives are likely to be lead compounds for a new class of anti-HCV agents.

4. Discussion

In the present study, we prepared a natural product library consisting of approximately 300 isolated compounds derived from fungi extract [17]. Among these compounds, we focused on sulochrin, which reduced HCV infectivity in the HCVcc system. Sulochrin suppressed the viral entry efficiencies both in the HCVpp and the HCVtcp systems, suggesting that this compound blocked HCV envelope-mediated entry. HCV was reported to enter host cells through clathrin-dependent endocytosis after engagement to host receptors [24–27]. Sulochrin is not likely to be a general inhibitor of clathrin-dependent endocytosis, but rather is specific for HCV entry, as it did not affect the entry of other viruses such as VSVpp and HBV, which were reported to enter by clathrin-dependent manners [28,29].

Sulochrin inhibits eosinophil degranulation, activation, and chemotaxis [30,31]. It also inhibits VEGF-induced tube formation of human umbilical vein endothelial cells [32]. In addition, 3-*O*-methylfunicone, a sulochrin derivative possessing anti-HCV activity, has an anti-tumor activity [33]. It is unknown if these activities of the compounds are related to their anti-HCV activity. The establishment of drug-resistant virus and the identification of the target molecule are in progress to reveal the mechanism of action of sulochrin and its derivatives. However, the present study is the

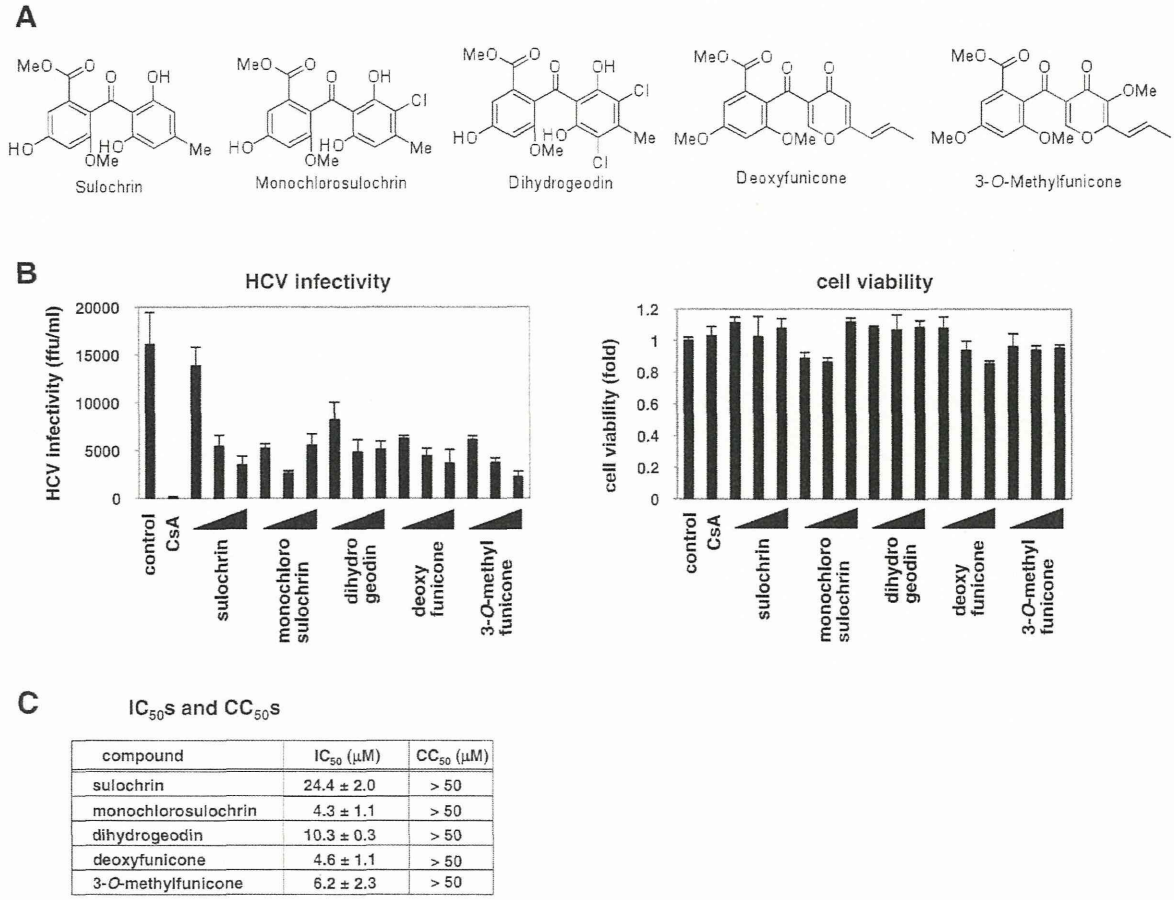

C

IC_{50}s and CC_{50}s

compound	IC_{50} (μM)	CC_{50} (μM)
sulochrin	24.4 ± 2.0	> 50
monochlorosulochrin	4.3 ± 1.1	> 50
dihydrogeodin	10.3 ± 0.3	> 50
deoxyfunicone	4.6 ± 1.1	> 50
3-*O*-methylfunicone	6.2 ± 2.3	> 50

Fig. 4. Derivative analysis of sulochrin. (A) Chemical structures of sulochrin derivatives examined in this study, monochlorosulochrin, dihydrogeodin, deoxyfunicone, 3-*O*-methyfunicone, as well as sulochrin. (B) Anti-HCV effects of the sulochrin derivatives (10, 30, and 50 μM) were investigated as shown in Fig. 1C. (C) The IC_{50} and CC_{50} values of the sulochrin derivatives are shown.